Complementary Analysis of Peptide Aggregation by NMR and Time-Resolved Laser Spectroscopy

Shawn L. Mansfield, Albert J. Gotch, Greg S. Harms, Carey K. Johnson, and Cynthia K. Larive*

Department of Chemistry, University of Kansas, Lawrence, Kansas 66045

Received: August 25, 1998; In Final Form: December 31, 1998

Aggregation is an important area of scientific investigation because of the consequences of this process for many aspects of protein and peptide chemistry. Previous studies of the aggregation of the βA4 peptide fragment, β(12−28), and synthetic analogues in low pH aqueous solution show that replacing either or both phenylalanines with glycine reduces the tendency of this peptide to form aggregates. In this investigation, several β(12−28) analogues have been synthesized in which the phenylalanine residues 19 and/or 20 have been substituted with the nonnative amino acid, naphthylalanine, to produce the peptides [napAla^{19,20}], [napAla^{19},Gly^{20}], and [Gly^{19},napAla^{20}] and allowing the aggregation behavior of these peptides to be examined in aqueous solution at low pH with both NMR and fluorescence spectroscopy. The NMR chemical shift, diffusion coefficients and relaxation times as well as rotational correlation times measured with both NMR and fluorescence spectroscopy are concentration dependent providing evidence that [napAla^{19,20}]β(12−28) forms soluble aggregates. Similar results obtained for [napAla^{19},Gly^{20}]β(12−28) and [Gly^{19},napAla^{20}]β(12−28) suggest that these peptides have a greatly reduced tendency to aggregate. In addition, [napAla^{19,20}]β(12−28) produces excimer fluorescence emission in a concentration-dependent manner with essentially no excimer detected in the fluorescence spectra of the singly substituted naphthylalanine analogues. Fluorescence lifetimes were measured, and unlike naphthylalanine, the free amino acid, the excimer fluorescence decay of [napAla^{19,20}]β-(12−28) does not exhibit a rise time component, suggesting a ground-state preassociation of the peptides through naphthyl $\pi-\pi$ interactions that stabilize the aggregates. Fluorescence spectroscopy, due to its concentration sensitivity, permits measurements of peptide solutions at much lower concentration than NMR, allowing direct measurement of the peptide monomer. However, NMR spectroscopy, through the measurement of nuclear relaxation times, can provide complementary information about the differential regional mobility of the peptide. The application of both NMR and fluorescence spectroscopy to the analysis of these naphthyl-substituted peptides produces a more complete picture of their aggregation behavior than could be obtained using either method alone. An advantage of using the combination of these methods is that their different time scales make them sensitive to different ranges of molecular motion.

Introduction

The aggregation of peptides and proteins is an important area of research because of its effect on the stability, purification, and analysis of these systems.[1−6] In addition to complicating their study in vitro, aggregation can also cause conformational changes which can significantly alter the in vivo properties of peptides and proteins such as transport and biological activity.[7−9] The detection of aggregation is the most basic aspect of this problem. To understand and avoid aggregation additional information is required including: (1) how much aggregate has formed; (2) what is the nature of the aggregate (dimer, tetramer, etc.); (3) what portion of the primary structure is involved in aggregation; (4) what are the fundamental forces that are involved in producing and stabilizing the aggregates? Once known, answers to these questions can be used to devise a strategy to prevent aggregation where it is undesirable.

In a recent report, we examined the aggregation of a 17 residue fragment, β(12−28), VHHQKLVFFAEDVGSNK, of the Alzheimer's related βA4 peptide using pulsed-field gradient (PFG) NMR spectroscopy.[10] The central hydrophobic patch of β(12−28), defined by residues 17−21, is integral to the aggregation of the peptide in acidic aqueous solution. Although the aromatic side chains of the phenylalanine residues are necessary for aggregate formation, the possible role of $\pi-\pi$ interactions in the aggregation of β(12−28) was not previously investigated.[10]

On the basis of information presented in our earlier report, a family of peptide analogues has been designed specifically to address the role of $\pi-\pi$ interactions in the aggregation of this peptide. The phenylalanine residues 19 and 20 were replaced with glycine or with the nonnative amino acid 2-naphthylalanine (napAla) to produce three β(12−28) analogues, [napAla^{19,20}]β-(12−28), [napAla^{19},Gly^{20}]β(12−28), and [Gly^{19},napAla^{20}]β(12−28). The naphthyl group is a much better fluorescence probe than the phenyl group so that fluorescence spectroscopy, as well as NMR spectroscopy, can be employed as complementary analytical methods to study the aggregation behavior of these peptides. It is well-known that aromatic hydrocarbons are capable of forming an excited-state dimer or excimer. The

* Corresponding author. Telephone: (785) 864-4269. Fax: (785) 864-5396. Email: Clarive@ukans.edu.

10.1021/jp983504g CCC: $18.00
Published on Web 03/04/1999

fluorescence emission maximum of the excimer is red-shifted relative to that of the monomer and can be used to provide spectroscopic information unique to the dimer.[11]

Aggregation results in an increased hydrodynamic volume and, therefore, a decrease in the peptide translational and rotational diffusion coefficients. Because translational and rotational diffusion coefficients are related to molecular size and shape, their measurement can be used to elucidate the behavior of interacting systems such as membrane transport, micelle formation by surfactants, and molecular association.[12−15] PFG NMR is a well-established method for measuring translational diffusion coefficients.[16−18] The translational diffusion coefficient, D_t, is given by the Stokes−Einstein relationship

$$D_t = kT/6\pi\eta r F_t \quad (1)$$

where η is solvent viscosity, r is hydrodynamic radius, and F_t is the translational frictional coefficient ratio.

The rotational diffusion coefficient is given by the relationship

$$D_r = kT/6V\eta F_r \quad (2)$$

where V is the hydrodynamic volume, η is solvent viscosity, and F_r is the frictional coefficient for rotation. The rotational diffusion coefficient can be determined by the measurement of the rotational correlation time, τ_c, which is related to the rotational diffusion coefficient of a spherical rotor by the simple equation

$$\tau_c = (6D_r)^{-1} \quad (3)$$

The rotational correlation time of a molecule can be measured with both NMR and fluorescence spectroscopy and used to characterize intermolecular interactions such as those associated with aggregate formation.

Molecular interactions can also be investigated through the analysis of NMR relaxation times. Both longitudinal and transverse relaxation processes are dependent on fluctuations caused by molecular motion and reflect changes in the apparent size of the molecule caused by interactions with other molecules. For dipolar relaxation of protons in a spherical molecule, the longitudinal (T_1) and transverse (T_2) relaxation times are related to the molecular rotational correlation time through the equations for the spectral density functions.[19] Aggregation-induced changes in molecular motion can be monitored as a function of amino acid residue to reveal differences in regional relaxation. In liquids, the predominant mechanism for proton relaxation is dipolar interactions. Using this assumption, rotational correlation times can be calculated from nuclear relaxation times for all nuclei that give rise to resolved resonances.[20] Concentration-dependent changes in relaxation can provide information about regional motion and/or individual group mobility and reveal the portion of the primary structure involved in the interaction. However, a limitation of NMR in the study of aggregation is the characteristically low concentration sensitivity, which may preclude the measurement of the monomeric species.[10]

Fluorescence spectroscopy is also well established for the analysis of molecular interactions.[21−28] Rotational correlation times can be obtained using time-resolved fluorescence anisotropy measurements, although this method is limited to molecules with a fluorescent label.[21,24−27] Additional information about the aggregation of the peptide can be extracted from steady-state fluorescence experiments if the concentration-dependent fluorescence intensity or emission maximum of the fluorophore is altered by aggregation, particularly through excimer formation. In this work, the use of both NMR and fluorescence spectroscopy produces a more complete picture of the aggregation behavior of these naphthyl-substituted peptide analogues than could be obtained using either analytical method alone.

Experimental Section

Sample Preparation. The peptides [napAla^{19,20}]β(12−28), [napAla^{19},Gly^{20}]β(12−28), and [Gly^{19},napAla^{20}]β(12−28) were prepared by solid-phase synthesis[29] in the University of Kansas Biochemical Research Service Laboratory employing FMOC (9-fluorenylmethoxycarbonyl) chemistry.[30] The peptides were purified with preparative reverse-phase HPLC, and their purity was verified with analytical reverse-phase HPLC. The structures were confirmed using ^{1}H NMR and MALDI or ESI-MS. Samples for NMR analysis were dissolved in D_2O, and the pD of the solution was adjusted to approximately 2.9 using DCl or NaOD. Samples for the fluorescence experiments were dissolved in H_2O and the pH was adjusted to approximately 2.8 with either HCl or NaOH. All experiments were performed at 25 °C.

Peptide Concentration Determination. Peptide aggregation is a concentration-dependent process, which requires the peptide concentration to be precisely determined to ascertain its behavior. Quantitative analysis was performed for a stock peptide solution using NMR spectroscopy by comparing the relative integrals of the peptide to a secondary standard of maleic acid sealed inside a capillary, as described previously.[31] From this stock peptide solution, five standard solutions from 10 to 200 μM were prepared, and the molar absorptivity, ϵ, of these peptides was determined at 277 nm by plotting absorbance against concentration. The values of ϵ used in the determination of the peptide concentrations were 5.75×10^3, 5.74×10^3, and 1.30×10^4 M^{-1} cm^{-1} for [napAla^{19},Gly^{20}]β(12−28), [Gly^{19},napAla^{20}]β(12−28), and [napAla^{19,20}]β(12−28), respectively.

NMR Measurements. One-dimensional ^{1}H NMR spectra for chemical shift analysis were measured with a Bruker AM-500 MHz NMR spectrometer for 95 μM, 0.95 mM, and 2.05 mM peptide solutions to monitor concentration-dependent changes in chemical shift. A capillary containing the chemical shift standard, 3-(trimethylsilyl)propionic-2,2,3,3-d_4 acid, sodium salt (TSP), was used as an external chemical shift reference. The two-dimensional ^{1}H NMR experiments TOCSY and NOESY were acquired with a Bruker DRX-400 spectrometer at 283 K using peptide solutions in 90% H_2O/10% D_2O at pH 2.8 and employed in the resonance assignments of [napAla^{19,20}]β(12−28).

Translational diffusion coefficients were extracted from BPPLED NMR spectra acquired with a Bruker AM-360 spectrometer equipped with an actively shielded z-gradient ^{1}H probe.[32] The gradient instrumentation has been described elsewhere.[33] The samples were placed in a cylindrical microcell to restrict diffusion to the linear region of the gradient coil. The value of I_0 was determined from the semilogarithmic plot of the integrated intensity and the square of the gradient amplitude. Diffusion coefficients were extracted by a NLSQ fit of a single-parameter model to resonance intensity using the program Scientist (Micromath).

All samples for the relaxation measurements were degassed to remove dissolved oxygen by performing three cycles of the freeze−pump−thaw procedure. NMR relaxation measurements were performed with a Bruker DRX-400 spectrometer using the inversion recovery and Carr−Purcell−Meiboom−Gill pulse sequences.[34,35] Longitudinal relaxation times were calculated from the spectral data by a three-parameter NLSQ fit of the

integrated intensities to compensate for 180° pulse imperfections.[36] The T_2 relaxation times were determined from the two-parameter NLSQ fit of the integrated resonance intensities. The error of these measurements is limited by the precision of the resonance integrals, approximately 5%.

Because dipolar interactions are the dominant relaxation mechanism for protons in liquids, the rotational correlation time, τ_c, may be calculated for the nuclei that give rise to resolved resonances by the following relationship:[20]

$$\tau_c\,(\mathrm{ns}) = a_0 + a_1(T_2/T_1) + a_2(T_2/T_1)^2 + a_3(T_2/T_1)^3 + a_4(T_2/T_1)^4 \quad (4)$$

where a_0-a_4 are coefficients that depend only on magnetic field strength and T_1 and T_2 are the longitudinal and transverse relaxation times, respectively.

Absorption and Steady-State Fluorescence Measurements. The steady-state excitation and emission spectra were acquired using a Photon Technology International QuantaMaster Luminescence Spectrometer with an excitation and emission bandpass of approximately 1 nm. A quartz 1.5 × 10 mm fluorescence microcell (Helma) was used in all experiments. UV absorption spectra were measured with a HP 8450A diode array spectrophotometer using quartz cells with path lengths of 1 cm, 1 mm, or 1 μm depending on the concentration of the peptides analyzed.

Time-Resolved Fluorescence Measurements. Time-resolved measurements were made with a time-correlated single photon counting (TCSPC) system described previously.[37] No effort was made to remove dissolved oxygen from these samples. The fluorescence excitation pulse was provided by a cavity-dumped rhodamine 6G dye laser, synchronously pumped by the second harmonic from a mode-locked Nd:YAG laser (Coherent Antares). The dye laser output at 574 nm was frequency doubled for fluorescence excitation. The monomer emission was collected at 328 nm and excimer emission at 450 nm.

Isotropic intensity decays (I_{MA}) were measured independent of rotational motion by setting the emission polarizer to the magic angle, 54.7° from vertical. Fluorescence anisotropy decays were obtained from the emission polarized parallel, $I_{||}$, and perpendicular, $I_{\perp}$, to the excitation polarizer. The rotational correlation times were determined by analysis of the $I_{||}$ and $I_{\perp}$ polarized fluorescence decays with reconvolution analysis software.[38] In fitting the anisotropy decay, the value of the initial anisotropy, r_0, was the most critical parameter due to the low initial anisotropy of the naphthyl-substituted peptides. Therefore, the initial anisotropy was determined in a separate time-resolved experiment with peptide solutions in propylene glycol at 0 °C. The long rotational correlation time in this solvent leads to an accurate determination of r_0 from a fit to the polarized fluorescence decays. These measurements were used to fix r_0 in the room-temperature anisotropy analysis.

Results

From prior knowledge that the $\beta(12-28)$ phenylalanine side chains are a primary driving force in the hydrophobic aggregation of this peptide[10,39] and the hypothesis that $\pi-\pi$ interactions may stabilize the aggregates, a family of peptide analogues of $\beta(12-28)$ was synthesized in which glycine and the nonnative amino acid 2-naphthlyalanine were substituted for one or both phenylalanine residues in the native peptide sequence. As a result of their improved fluorescence characteristics, the aggregation behavior of these naphthylalanine-substituted peptides can be studied by both NMR and fluorescence spectroscopy. These complementary methods allow the determination of translational diffusion coefficients and molecular rotational correlation times, which can be used as probes of hydrodynamic size. Fluorescence spectroscopy, due to its concentration sensitivity, permits measurements of peptide solutions at much lower concentration than NMR, allowing direct measurement of the peptide monomer. However, NMR spectroscopy, through the measurement of nuclear relaxation times, can provide complementary information about the differential regional mobility of the peptide.

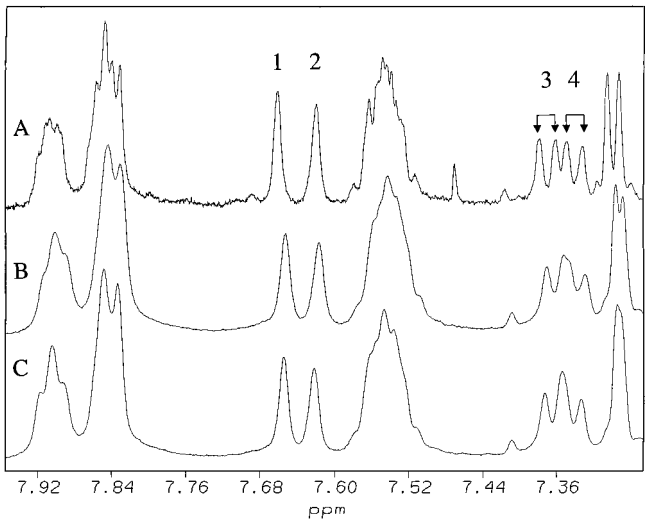

Figure 1. ^{1}H NMR spectra of the aromatic region of the [napAla^{19,20}]β-(12−28) peptide in D_2O at (a) 0.095 mM, (b) 0.95 mM, and (c) 2.05 mM. Specific assignments are provided for the numbered peaks: (1) napAla^{20} 1H; (2) napAla^{19} 1H; (3) napAla^{20} 3H; (4) napAla^{19} 3H.

Concentration Dependence of NMR Chemical Shifts. The chemical shifts of nuclei are fundamentally dependent on their environment; therefore, changes in the local environment are reflected in the resonance chemical shift. Qualitative evidence supporting the hypothesis that the naphthyl rings stabilize the peptide aggregates can be observed in the concentration dependence of the chemical shifts of the naphthyl ring protons. The concentration dependence of the [napAla^{19,20}]$\beta(12-28)$ naphthyl aromatic chemical shifts can be discerned from the ^{1}H NMR spectra shown in Figure 1. Although subtle differences in chemical shift (<2 Hz) were also observed for some resonances in other spectral regions, the napAla^{20} 1H and 3H protons were the most significantly affected. However, the observed chemical shift changes are insufficient to permit quantitative analysis of the aggregation behavior of the peptide.

NMR Translational Diffusion Coefficients. The translational diffusion coefficients were measured at a high (2.0 mM), low (0.5 mM), and intermediate concentration for each of the naphthylalanine-substituted peptides in acidic D_2O solution. The diffusion coefficients of all three peptides are invariant within the concentration range measured, and these results are (1.99 ± 0.02) × 10^{-10}, (2.40 ± 0.06) × 10^{-10}, and (2.26 ± 0.02) × 10^{-10} m^2/s for the [napAla^{19,20}]$\beta(12-28)$, [Gly^{19},napAla^{20}]β-(12−28), and [napAla^{19},Gly^{20}]$\beta(12-28)$ peptides, respectively. The invariance of the translational diffusion coefficient of these peptides is indicative of a constant hydrodynamic volume over this concentration range and thus a constant aggregation state. The substitution of a glycine at residue 19 or 20 results in an increase in the peptide diffusion coefficient relative to that of [napAla^{19,20}]$\beta(12-28)$ reflecting a reduction in the extent of aggregation. These studies are consistent with the reduction or

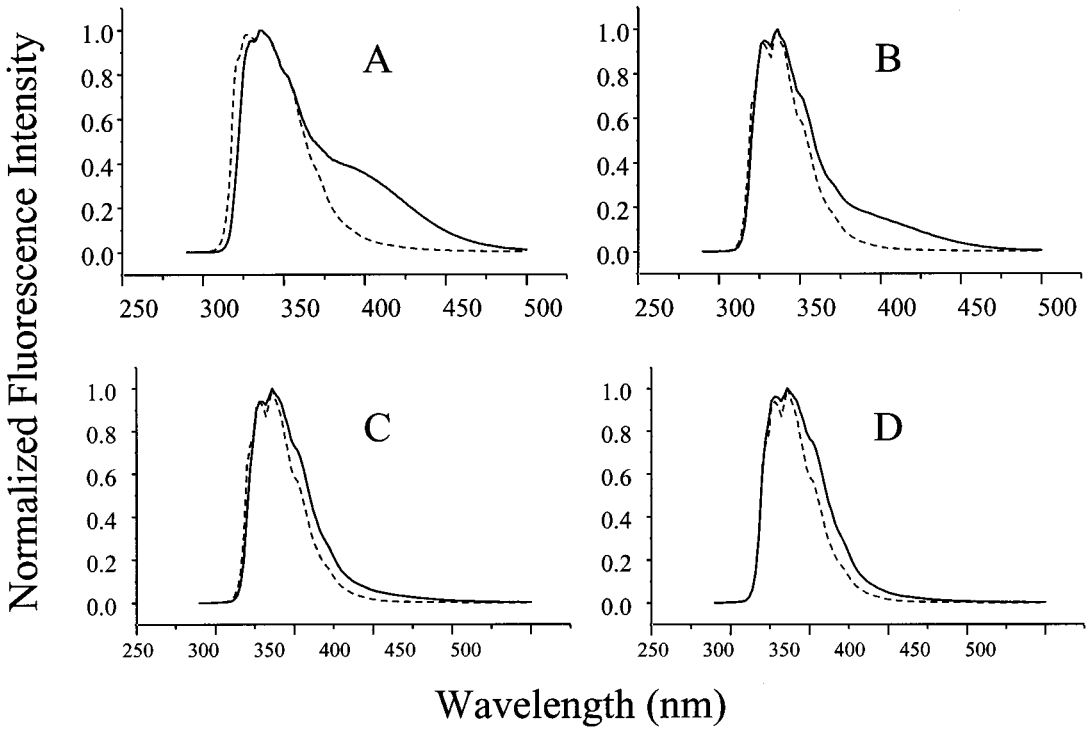

Figure 2. Steady-state fluorescence spectra (not corrected for self-absorption) of (a) [napAla^{19,20}]β(12−28) peptide (- - -) at 0.1 mM and (—) at 2.5 mM; (b) 2-naphthylalanine (- - -) at 0.1 mM and (—) at 4.5 mM; (c) [napAla^{19},Gly^{20}]β(12−28) peptide (- - -) at 0.1 mM and (—) at 3.0 mM; (d) [Gly^{19},napAla^{20}]β(12−28) peptide (- - -) at 0.1 mM and (—) at 3.0 mM.

elimination of aggregation in β(12−28) peptide analogues in which glycine was substituted for phenylalanine residues 19 and/or 20.[10] The results also support the observation of Esler et al. that replacement of Phe^{19} with Thr transforms the plaque-competent β(10−35) into a plaque-incompetent peptide.[39] These results suggest that substitution of a glycine residue at position 19 may be more disruptive to aggregation than at position 20 as reflected in the slower diffusion of [napAla^{19},Gly^{20}]β(12−28).

Absorption and Steady-State Fluorescence Experiments. Because of the importance of the phenylalanine residues for the hydrophobic aggregation of the β(12−28), it was hypothesized that the substitution of these residues with naphthylalanine would stabilize the aggregate through an increased hydrophobic surface and facilitate excimer formation. To investigate this possibility, steady-state fluorescence experiments were performed with aqueous solutions of [napAla^{19,20}]β(12−28) ranging in concentration from 50 μM to approximately 2.5 mM (Figure 2a). The emission spectrum of the peptide is similar to that of 2-naphthylalanine (2-napAla), the free amino acid (Figure 2b). At the lowest concentrations, the fluorescence spectra of 2-napAla and [napAla^{19,20}]β(12−28) contain a single broad band centered at 328 nm. In more concentrated solutions of 2-napAla and [napAla^{19,20}]β(12−28), a red-shifted excimer band centered at 420 nm is observed in the fluorescence emission spectra. The absence of this excimer band at low concentrations indicates that the excimer is formed through intermolecular interactions because the formation of an intramolecular excimer by [napAla^{19,20}]β(12−28) would not be concentration independent. Similar experiments performed on solutions of [napAla^{19},Gly^{20}]β(12−28), and [Gly^{19},napAla^{20}]β(12−28) (Figure 2c,d) show essentially no excimer fluorescence. Ground-state absorption spectra were measured with UV spectroscopy for these solutions and no changes were detectable, suggesting that the naphthyl groups may not be close enough to perturb the electronic structure.

Fluorescence Lifetime Measurements. To further characterize excimer formation, fluorescence lifetimes of 50 μM and 2.0 mM solutions of 2-napAla and the naphthylalanine-substituted peptides were measured for the monomer emission at 328 nm and the excimer emission at 450 nm. Parameters derived from fits of the fluorescence decays are given in Table 1. The major component of the peptide fluorescence lifetimes remains essentially constant, suggesting that the electronic structure of the naphthyl rings are not significantly perturbed by aggregation. This result is in agreement with the findings of Mataga et al., who reported no concentration dependence in the fluorescent lifetimes of alkylnaphthalene derivatives.[40] The variations of the minor components might reveal interesting results, but a detailed analysis of fluorescence lifetimes is outside the scope of this work.

The fluorescence decay of the intermolecular excimer emission normally includes a rise time component because of the diffusive nature of excimer formation[41] as indicated in the excimer fluorescence decay of the free amino acid 2-naphthylalanine, shown in Figure 3b. The fluorescence decay of the [napAla^{19,20}]β(12−28) excimer emission (Figure 3a) does not include a resolvable rise time, indicating that a preassociative ground-state complex (aggregate) is stabilized by intermolecular $\pi-\pi$ interactions between naphthyl groups.

Rotational Correlation Time Measurements. Time-resolved fluorescence anisotropy measurements were performed using the monomer fluorescence to determine the rotational correlation times, τ_c, of this peptide family at 50 μM and 2.0 mM and are reported in Table 2. The polarized fluorescence decays were fitted to a single rotational correlation time with $\chi^2 \leq 2.5$ for all fits. Attempts were made to extract the excimer rotational correlation time from the excimer fluorescence decay, but the initial anisotropy is too close to zero to allow an acceptable analysis of the data. The rotational correlation times measured for both concentrations of [napAla^{19},Gly^{20}]β(12−28) and [Gly^{19},napAla^{20}]β(12−28) are identical within the confidence limits.

TABLE 1: Fluorescence Lifetime Parameters of Naphthyl-Substituted Peptides and 2-Naphthylalanine

		328 nm				
	[peptide] (nm)	τ_1 (ns)	α_1	τ_2 (ns)	α_2	χ^2
[napAla^{19,20}]β(12−28)	0.05	38.2	0.888	1.6	0.112	1.7
	2.00	38.2	0.774	4.3	0.226	1.8
[napAla^{19},Gly^{20}]β(12−28)	0.05	40.3	0.965	6.0	0.035	2.0
	2.00	41.4	0.922	1.4	0.078	2.2
[Gly^{19},napAla^{20}]β(12−28)	0.10	41.1	0.608	1.4	0.346	2.4
	3.00	41.7	0.846	1.3	0.154	1.8
2-naphthylalanine	4.50	38.4	0.671	15.3	0.329	2.0

		450 nm						
	[peptide] (mM)	τ_1 (ns)	α_1	τ_2 (ns)	α_2	τ_3 (ns)	α_3	χ^2
[napAla^{19,20}]β(12−28)	0.05	39.8	0.091	6.8	0.388	1.8	0.522	1.3
	2.00	55.9	0.195	8.1	0.437	1.6	0.373	1.6
2-naphthylalanine	4.50	37.7	0.500	18.3	−0.460	1.4	0.040	1.5

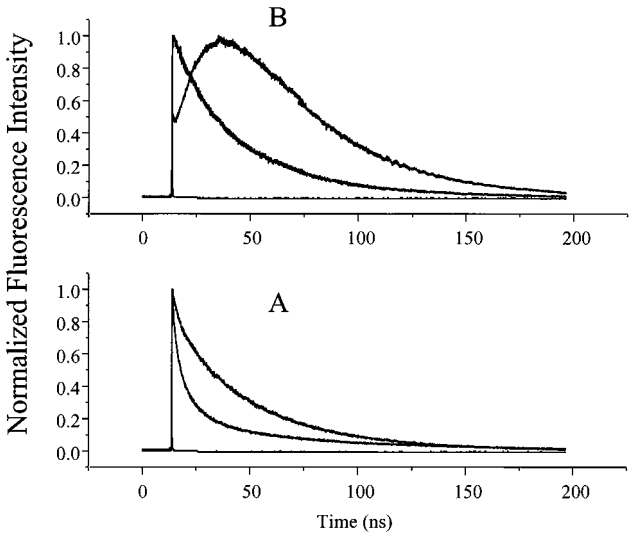

Figure 3. Time-resolved fluorescence decays of (a) [napAla^{19,20}]β-(12−28) peptide and (b) 2-naphthylalanine. In (a), the slow decay is the monomer fluorescence emission decay and the fast decay is the excimer fluorescence emission decay. In (b), the single decay is the monomer fluorescence emission decay, while the decay with the rise time is the excimer fluorescence emission decay. In both graphs, the instrument response is plotted but is too short to visualize. The monomer emission was detected at 328 nm and that of the excimer at 450 nm.

TABLE 2: Rotational Correlation Times Obtained from Time-Resolved Fluorescence Anisotropy at 328 nm

analyte	concn (mM)	r_0	τ_c (ps)[a]	90% confidence limits (ps)	χ^2
[napAla^{19,20}]β(12−28)	0.05	0.085	510	130	1.2[1]
	2.00	0.085	1510	490	1.7
[Gly^{19}, napAla^{20}] β(12−28)	0.05	0.088	530	160	2.0
	2.00	0.088	510	180	0.6
[napAla^{19},Gly^{20}] β(12−28)	0.05	0.101	590	180	2.5
	2.00	0.101	520	180	0.8
2-naphthylalanine	0.05	0.141	72	18	1.4

[a] Uncertainties in τ_c were estimated by the F-test which was used to compare χ^2 values at the 90% confidence limit.[44]

In addition, this rotational correlation time is identical within experimental error to the τ_c determined for the 50 μM [napAla^{19,20}]β(12−28) solution. The roughly three-fold increase in the rotational correlation time of the peptide at high concentration results from aggregation. The anisotropy decay curves for 50 μM and 2.0 mM solutions of [napAla^{19,20}]β(12−28) are clearly different, as shown in Figure 4.

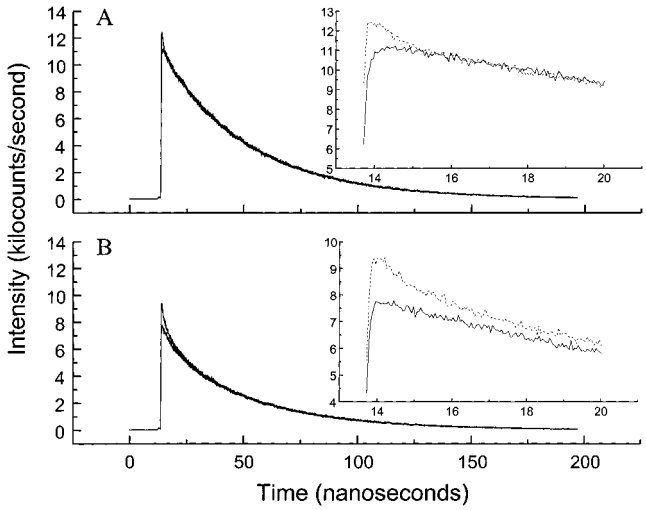

Figure 4. Time-resolved anisotropy decays for the [napAla^{19,20}]β(12−28) peptide at (a) 0.05 mM and (b) 2.0 mM. The solid line represents $I_\perp$, and the dashed lines represent $I_\parallel$ for both decays. The inset axes have the same units.

NMR Relaxation and Rotational Correlation Times. NMR relaxation times can indicate the location of the interaction site in the aggregates due to the reduction of mobility, hence, the nuclear relaxation rates of the interacting residues. The longitudinal and transverse relaxation times were measured for 0.5 and 2.0 mM peptide solutions. Because of the high degree of spectral overlap, relaxation times could be determined only for the protons that give rise to well-resolved resonances, generally in the aromatic and methyl regions of the ^{1}H NMR spectra. Compared with the peptides containing a single naphthylalanine substitution, the methyl group resonances of the [napAla^{19,20}]β-(12−28) peptide are relatively well resolved as a result of the close proximity of the naphthyl rings. Therefore, the methyl protons of [napAla^{19,20}]β(12−28) can provide additional information about the intermolecular interactions associated with aggregate formation. Of the [napAla^{19,20}]β(12−28) aromatic protons, only the 1H resonances of both naphthylalanines are sufficiently well resolved to allow measurement of the relaxation times. The relaxation times of the 1H and 3H aromatic protons of the [Gly^{19},napAla^{20}]β(12−28) and [napAla^{19},Gly^{20}]β(12−28) peptides are invariant with concentration, as shown in Table 3. However, the T_1 and T_2 relaxation times of the resolved hydrophobic side chain resonances of the [napAla^{19,20}]β(12−28) peptide decrease significantly with increasing concentration.

The rotational correlation times of the naphthyl groups of these peptides were calculated from the NMR relaxation

TABLE 3: NMR Relaxation and Correlation Times of Selected Protons of the [napAla^{19,20}]β(12−28), [napAla^{19}, Gly^{20}]β(12−28), and [Gly^{19},napAla^{20}]β(12-28) Peptides in D_2O Solution at Low pH

residue	concn (mM)	T_1 (s)	T_2 (s)	τ_c (ps)
	[napAla^{19,20}]β(12−28)			
Val^{18} CH_3	0.43	0.36	0.15	400
	1.57	0.26	0.07	680
Val^{18} CH_3	0.43	0.44	0.21	340
	1.57	0.29	0.08	610
napAla^{19} 1H	0.43	1.0	0.34	520
	1.57	0.42	0.12	610
napAla^{20} 1H	0.43	0.86	0.31	490
	1.57	0.41	0.11	680
Ala^{21} CH_3	0.43	0.42	0.23	280
	1.57	0.33	0.14	400
Val^{24} CH_3	0.43	0.45	0.22	340
	1.57	0.30	0.11	490
Val^{24} CH_3	0.43	0.44	0.24	290
	1.57	0.31	0.12	430
	[napAla^{19},Gly^{20}]β(12−28)			
napAla 1H	0.63	1.4	0.53	450
	2.36	1.4	0.52	470
napAla 3H	0.63	1.6	0.81	330
	2.36	1.6	0.61	440
	[Gly^{19},napAla^{20}]β(12−28)			
napAla 1H	0.55	1.3	0.49	440
	2.29	1.3	0.51	450
napAla 3H	0.55	1.4	0.56	470
	2.29	1.6	0.58	450

parameters using eq 4 and are reported in Table 3. With the exception of the [napAla^{19},Gly^{20}]β(12−28) napAla 3H proton, the NMR rotational correlation times of the [napAla^{19},Gly^{20}]β-(12−28) and [Gly^{19},napAla^{20}]β(12−28) aromatic protons measured as a function of concentration are invariant within experimental error and are similar in magnitude to the rotational correlation times measured with fluorescence spectroscopy for the same peptide species. The correlation times of the aromatic protons of [napAla^{19,20}]β(12−28) are similar to those measured for the peptides with a single naphthylalanine substitution at the lower concentration studied (0.43 mM) but are larger at the higher concentration (1.57 mM). As a result of propagation of error from the relaxation times, the estimated error of the calculated correlation times is relatively large, approximately 10%. Also, because the calculation of correlation times is based on the assumption that the fraction of the dipolar contribution is essentially the same for both the T_1 and T_2 relaxation mechanisms, it is also possible that a change in the available relaxation pathways as a result of aggregation could contribute to the error in the calculated correlation times at the higher concentrations. However, even taking these limitations into account, the correlation times measured for the [napAla^{19,20}]β-(12−28) methyl and aromatic protons all increase with increasing peptide concentration, revealing a trend that supports the other evidence that this peptide is aggregating.

Discussion

The objectives of this research were to determine the elements of primary structure involved in the intermolecular interactions responsible for aggregation and to elucidate the fundamental forces that result in aggregation. Furthermore, the use of these two complementary analytical techniques has provided more information about the aggregation of this peptide family than could be obtained from a single analytical approach.

In contrast to our previous study of the aggregation of β-(12−28), the [napAla^{19,20}]β(12−28) peptide diffusion coefficient is not concentration dependent, probably because the larger aromatic rings increase the stability of the aggregate, shifting the equilibrium toward dimer formation. Even so, the translational diffusion coefficients reveal differences in the hydrodynamic volumes that can be interpreted qualitatively in terms of the aggregation state by comparison with previously published results for β(12−28) analogues.[10] The diffusion coefficient determined for [napAla^{19,20}]β(12−28), $(1.99 \pm 0.02) \times 10^{-10}$ m^2/s, is similar to the value reported for a 3.24 mM β(12−28) peptide solution, $(2.04 \pm 0.03) \times 10^{-10}$ m^2/s, indicating that the dinaphthyl-substituted peptide is predominately aggregated, probably as the dimer, over the concentration range studied.[10] However, the diffusion coefficient of [napAla^{19,20}]β(12−28) is somewhat faster than the diffusion coefficient reported for the covalently linked dimer, ([Cys^{20}]β(12−28))$_2$, $(1.78 \pm 0.03) \times 10^{-10}$ m^2/s.[10] This difference may be attributed to some contribution of monomeric peptide to the [napAla^{19,20}]β(12−28) diffusion coefficient or to the formation of a more compact dimeric structure by [napAla^{19,20}]β(12−28). An increase of hydrodynamic volume resulting from [napAla^{19,20}]β(12−28) dimer formation might be partially compensated by a lower friction coefficient due to a more compact shape. The diffusion coefficient of [Gly^{19},napAla^{20}]β(12−28), $(2.40 \pm 0.06) \times 10^{-10}$ m^2/s, is similar to the value previously reported for the nonaggregating [Gly^{19,20}]β(12−28) peptide, $(2.48 \pm 0.04) \times 10^{-10}$ m^2/s suggesting that this peptide is predominately monomeric. The intermediate diffusion coefficient of [napAla^{19},-Gly^{20}] β(12−28) peptide, $(2.26 \pm 0.02) \times 10^{-10}$ m^2/s, suggests that dimer may be present in solutions of this peptide, although neither the fluorescence or NMR relaxation measurements support this view.

Although these results provide a qualitative guide to the analysis of the aggregation behavior of these peptides, they also demonstrate the problems that can be encountered in using diffusion coefficients alone for the analysis of peptide aggregation. Because the hydrodynamic volume reflects not just the size but also the shape of a molecule, it is possible that the naphthyl substitutions result in subtle differences in conformation that are reflected in the diffusion coefficient. Perhaps the most significant limitation of this approach is the effective dynamic range of translational diffusion coefficients, which scale roughly as the cube root of the molecular weight, making them relatively insensitive indicators of the subtle changes in the distribution of monomeric and aggregated peptides.

The lack of a rise time component in the excimer fluorescence emission decay of [napAla^{19,20}]β(12−28) with an experimental resolution of 20 ps indicates that any structural reorganization required for the formation of the excimer occurs on an extremely short time scale, providing specific evidence that the peptide is aggregated prior to the excitation of the naphthyl ring. More importantly, the fast excimer formation time demonstrates the proximity of the naphthyl rings in the ground state, indicating that intermolecular $\pi-\pi$ interactions between naphthyl rings stabilize the aggregates. Additional evidence is provided for $\pi-\pi$ interactions by the concentration-dependent changes in NMR chemical shifts and rotational correlation times of the naphthylalanine aromatic protons.

Concerns that the excimer formed may be due to intramolecular naphthyl ring interactions are eliminated by the observed concentration dependence of the steady-state excimer fluorescence of [napAla^{19,20}]β(12−28) as shown in Figure 2. However, this observation does not eliminate the possibility that aggregation is accompanied by a conformational change that leads to the formation of an intramolecular excimer. Previous fluores-

cence studies of excimer formation have produced the "$n = 3$" rule, which states that the most favorable condition for intramolecular excimer formation occurs when the aromatic rings are separated by three atoms.[42,43] In [napAla^{19,20}]β(12−28), the aromatic rings are separated by four atoms, a less favorable condition for intramolecular excimer formation. In addition, the concentration dependence of the NMR relaxation measurements and correlation times is also consistent with the formation of an intermolecular contact involving the central hydrophobic residues, including the naphthylalanine rings.

Of the peptides examined, the naphthyl aromatic proton longitudinal relaxation times of only [napAla^{19,20}]β(12−28) change significantly over the concentration range studied. The longitudinal relaxation times of the methyl groups of residues Val^{18}, Ala^{21}, and Val^{24}, shown in Table 3, are affected by concentration, but the change is not as great as for the naphthyl aromatic protons, suggesting that the segmental mobility of the methyl groups of these residues is less affected by aggregation. From analysis of the concentration-dependent longitudinal relaxation times, a picture emerges in which the peptide is associated by contacts involving the central hydrophobic residues. This result is also consistent with the reduction of aggregation observed upon replacement of either naphthylalanine residue with glycine.

The T_2 relaxation times of the aromatic protons of the singly naphthyl-substituted peptides are equivalent within experimental error at both concentrations examined. However, the T_2 relaxation times of the aromatic and methyl group protons of [napAla^{19,20}]β(12−28) decrease significantly as the concentration is increased due to a reduction in local mobility as a result of aggregation. The concentration dependence of the T_2 relaxation times is also reflected in the concentration dependence of the resonance line widths in the spectra shown in Figure 1.

Although the relative decreases of T_1 and T_2 relaxation times with increasing concentration are greatest for the naphthyl aromatic protons, a larger change in the NMR correlation times is observed for the methyl protons. The equations that relate T_1 and T_2 to the correlation time are very similar, except that the T_2 relationship includes a zero-frequency spectral density term that makes it sensitive to low-frequency motions.[20] Therefore, the correlation times of the aromatic protons of [napAla^{19,20}]β-(12−28) presented in Table 3 are less affected by aggregation than are the relaxation times of the methyl protons.

The difference between the concentration-dependent changes in the fluorescence and the NMR rotational correlation times of the [napAla^{19,20}]β(12−28) aromatic protons may reflect a different sensitivity to localized motions. Anisotropy measurements by fluorescence detect mainly the overall rotation of the molecule, whereas the relaxation measurements of NMR are not only sensitive to overall motion but also to limited rotations (i.e., librations). This additional contribution to the relaxation, particularly for the naphthyl rings, can explain the smaller increase in the NMR rotational correlation time with concentration relative to the fluorescence results.

Use of eqs 1 and 2 permits the calculation of the hydrodynamic volume from both the translational diffusion coefficients and the fluorescence rotational correlation time, permitting direct comparison of the results of these measurements. Because the peptide does not assume a preferred conformation, the correct shape-dependent frictional parameters cannot be calculated. Therefore, the comparison can be made only on a relative basis because the volumes are calculated under the assumption that the peptide structure can be approximated as spherical. This introduces a bias into calculated hydrodynamic volumes but should not change the conclusions drawn on a relative basis. The diffusion coefficient of [napAla^{19,20}]β(12−28) is $1.99 \pm 0.02 \times 10^{-10}$ m^2/s, resulting in a hydrodynamic volume of $(4.20 \pm 0.13) \times 10^{-27}$ m^3. The rotational correlation time of [napAla^{19,20}]β(12−28) is 1510 ± 490 ps, which corresponds to a hydrodynamic volume of $(6.97 \pm 2.26) \times 10^{-27}$ m^3. These results agree well despite the fact that the measurements resulted from two totally different phenomena and that the translational diffusion coefficient may reflect some contribution from the monomer as a result of chemical exchange.

Conclusions

The [napAla^{19,20}]β(12−28) peptide appears to be a good model for understanding the aggregation of the β(12−28) peptide at low pH. The incorporation of naphthylalanine into this peptide allows the use of both NMR and fluorescence spectroscopy, demonstrating the power of employing complementary analytical methodologies for the study of peptide aggregation. The results presented collectively provide direct evidence that $\pi-\pi$ interactions between the naphthyl rings stabilize the peptide aggregate. In addition, the analysis of the NMR relaxation times provides insight into aggregation-dependent changes in local environment experienced by several of the [napAla^{19,20}]β(12−28) methyl protons. The results of the NMR translational diffusion and fluorescence rotational correlation times are in good agreement and suggest that the peptide forms a dimer at the higher concentrations studied. Although correlation times determined by the NMR and fluorescence measurements are in good agreement at lower concentrations, the NMR correlation times determined for a more concentrated solution of [napAla^{19,20}]β(12−28) are significantly lower than the value measured by fluorescence because the fluorescence rotational correlation times are insensitive to additional motions, such as librations, that affect NMR relaxation.

Acknowledgment. The authors gratefully acknowledge the support of the National Science Foundation Grants CHE 95-02389 (C.K.L. and S.L.M.) and CHE 93-21659 (A.J.G.). The 360 MHz NMR spectrometer used in this work was a generous gift from the Monsanto Company. The authors thank Dr. Michael Alterman for assistance with peptide synthesis and Dr. Steve Pauls for assistance with the TCSPC system.

References and Notes

(1) Brochon, J. C.; Tauc, P.; Merola, F.; Schoot, B. M. *Anal. Chem.* **1993**, *65*, 1028.
(2) Nohara, D.; Yamada, T.; Watanbe, A.; Tomoya, S. *Biotech. Bioeng.* **1994**, *44*, 276.
(3) Jaenicke, R. *Philos. Trans. R. Soc. London B* **1995**, *348*, 97.
(4) Taubes, G. *Science* **1996**, *271*, 1493.
(5) Chen, C.-C.; King, J.; Wang, D. I. C. *AIChE J.* **1995**, *41*, 1015.
(6) Mitraki, A.; Fane, B.; Haase-Pettingell, C.; Sturtevant, J.; King, J. *Science* **1991**, *253*, 54.
(7) Manning, M. C.; Patel, K.; Borchardt, R. T. *Pharm. Res.* **1989**, *6*, 903.
(8) Kralchevesky, P. A.; Paunov, V. N.; Denkov, N. D.; Nagayama, K. *J. Chem. Soc., Faraday Trans.* **1995**, *91*, 3415.
(9) Fields, G. B.; Alonso, D. O. V.; Stigter, D.; Dill, K. A. *J. Phys. Chem.* **1992**, *96*, 3974.
(10) Mansfield, S. L.; Jayawickrama, D. A.; Timmons, J. S.; Larive, C. K. *Biochim. Biophys. Acta* **1998**, *1382*, 257.
(11) Birks, J. B. *Photophysics of Aromatic Molecules*; John Wiley and Son, Ltd.: New York, 1970; Chapter 7, pp 301-371.
(12) Soderman, O.; Stilbs, P. *Prog. NMR Spectrosc.* **1994**, *26*, 445.
(13) Waldeck, A. R.; Kuchel, P. W.; Lennon, A. J.; Chapman, B. E. *Prog. NMR Spectrosc.* **1997**, *30*, 39.
(14) Lin, M.; Larive, C. K. *Anal. Biochem.* **1995**, *229*, 214.
(15) Orfi, L.; Lin, M.; Larive, C. K. *Anal. Chem.* **1998**, *70*, 1339.
(16) Veith, M.; Kolinski, A.; Skolnick, J. *Biochemistry* **1996**, *35*, 955.
(17) Callaghan, P. T. *Aust. J. Phys.* **1984**, *37*, 359.

(18) Everhart, C. H.; Johnson, C. S., Jr. *J. Magn. Reson*. **1982**, *48*, 466.
(19) Heatley, F. *Prog. NMR Spectrosc.* **1979**, *13*, 47.
(20) Carper, W. R.; Keller, C. E. *J. Phys. Chem. A* **1997**, *101*, 3246.
(21) Millar, D. P. *Curr. Opin. Struct. Biol*. **1996**, *6*, 637.
(22) Benson, D. R.; Fu, J. *Tetrahedron Lett.* **1996**, *37*, 4833.
(23) Chabbert, M.; Piémont, E.; Prendergast, F. G.; Lami, H. *Arch. Biochem. Biophys*. **1995**, *322*, 429.
(24) Visser, N. V.; van Hoek, A.; Visser, A. J. W. G.; Frank, J.; Apell, H.; Clarke, R. J. *Biochemistry* **1995**, *34*, 11777.
(25) Fa, M.; Karolin, J.; Aleshkov, S.; Strandberg, L.; Johansson, L. B.-Å.; Ny, T. *Biochemistry* **1995**, *34*, 13833.
(26) Delong, L. J.; Nichols, J. W. *Biophys. J*. **1996**, *70*, 1466.
(27) Han, Y.; Chaudhary, A. G.; Chordia, M. D.; Sackett, D. L.; Perez-Ramirez, B.; Kinston, D. G. I.; Bane, S. *Biochemistry* **1996**, *35*, 14173.
(28) Coutinho, A.; Prieto, M. *Biophys. J.* **1995**, *69*, 2541.
(29) Merrifield, R. B. *J. Am. Chem. Soc*. **1963**, *85*, 2149.
(30) Atherton, E.; Logan, C. J.; Sheppard, R. C. *J. Chem. Soc., Perkins Trans. 1* **1981**, 538.
(31) Larive, C. K.; Jayawickrama, D.; Orfi, L. *Appl. Spectrosc.* **1997**, *51*, 1531.
(32) Wu, D.; Chen, A.; Johnson, C. S., Jr. *J. Magn. Reson., Ser. A* **1995**, *115*, 260.
(33) Lin, M.; Jayawickrama, D. A.; Rose, R. A.; DelViscio, J. A.; Larive, C. K. *Anal. Chim. Acta* **1995**, *307*, 450.
(34) Kowalewski, J.; Levy, G. C.; Johnson, L. F.; Palmer, L. *J. Magn. Reson.* **1977**, *26*, 533.
(35) Meiboom, S.; Gill, D. *Rev. Sci. Instrum.* **1958**, *29*, 688.
(36) Sass, M.; Ziessow, D. J. *J. Magn. Reson.* **1977**, *25*, 263.
(37) Harms, G. S.; Pauls, S. W.; Hedstrom, J. H.; Johnson, C. K. *J. Fluoresc.* **1997**, *7*, 273.
(38) Cross, A. J.; Fleming, G. R. *Biophys. J.* **1984**, *46*, 46.
(39) Elser, W. P.; Stimson, E. R.; Ghilardi, J. R.; Lu, Y.; Felix, A. M.; Vinters, H. V.; Mantyh, P. W.; Lee, J. P.; Maggio, J. E. *Biochemistry* **1996**, *35*, 13914.
(40) Mataga, N.; Tomura, M.; Nishimura, H. *Mol. Phys.* **1965**, *9*, 367.
(41) Birks, J. B.; Dyson, D. J.; Munro, I. H. *Proc. R. Soc. A* **1963**, *275*, 575.
(42) Chandross, E. A.; Dempster, C. J. *J. Am. Chem. Soc.* **1970**, *93*, 3586.
(43) Hirayama, F. *J. Chem. Phys.* **1965**, *42*, 3163.
(44) Shoemaker, D. P.; Garland, C. W.; Nibler, J. W. *Experiments in Physical Chemistry*; McGraw-Hill: New York, 1996; pp 815−817.